SOLID STATE PHYSICS, VOLUME 48

Physical Properties of Metal-Doped Fullerene Superconductors

CHARLES M. LIEBER
ZHE ZHANG

Divisions of Applied Sciences and Department of Chemistry
Harvard University
Cambridge, Massachusetts

I. Introduction

The discovery of superconductivity in potassium-doped C_{60} at 18 K by Hebard and coworkers[1] was an unexpected observation that has caused an explosion of condensed matter research. In the brief two-year period since this report, the field of fullerene superconductivity has undergone a remarkable development with the identification of the superconducting phase in potassium-doped C_{60}, the discovery of new alkali metal–doped C_{60} materials having critical transition temperatures (T_c) exceeding 30 K, and the elucidation of many of the key normal and superconducting state properties of these materials.[2,3] Furthermore, the alkali metal–doped fullerenes now represent the highest-T_c molecular superconductor, and were it not for the discovery of superconductivity in copper oxide

[1]A. F. Hebard, M. J. Rosseinsky, R. C. Haddon, D. W. Murphy, S. H. Glarum, T. T. M. Plastra, A. P. Ramirez, and A R. Kortan, *Nature* **350,** 600 (1991).
[2]A. F. Hebard, *Physics Today* **45,** 26 (1992).
[3]R. C. Haddon, *Accts. Chem. Res.* **25,** 127 (1992).

ISBN 0-12-607748-7
ISBN 0-12-606048-7 (pbk.)

materials several years earlier they would be the highest-T_c superconductors, period.

The key component of the fullerene superconductors is the molecular cluster C_{60}, or Buckminsterfullerene. C_{60} and other fullerene clusters were first detected experimentally in the mass spectroscopy studies of Smalley and coworkers.[4–10] To reconcile the unusual stability of the C_{60} cluster, Smalley and coworkers proposed that the 60 carbon atoms formed a truncated icosahedron (soccer ball) structure in which each of the 60 carbon atoms was equivalent (Fig. 1).

The name Buckminsterfullerene (C_{60}) or, more generally, fullerene to describe the family of carbon clusters (e.g., C_{60}, C_{70}, C_{84} . . .) comes from the architect R. Buckminster Fuller whose geodesic domes inspired the original structure proposal for C_{60}.[11] The original techniques used by Smalley and others to generate fullerenes for their gas phase studies did not produce isolable quantities of C_{60} and thus were inadequate for materials research. This situation changed rapidly, however, with the development by Krätschmer and Huffman[12] of a simple method for preparing macroscopic quantities of C_{60} [for details see "Preparation of Fullerenes and Fullerene-Based Materials" in this volume]. This synthetic development represents a key advance, since it has been the availability of large quantities of pure, solid C_{60} that has fueled the explosion of research in this field. In addition to the fullerene-based superconductors, which represent the focus of this chapter, materials exhibiting interesting optical and magnetic properties are also emerging from this work.[13–17]

In this chapter we will review the field of fullerene superconductivity

[4]H. W. Kroto, J. R. Heath, S. C. O'Brien, R. F. Curl, and R. E. Smalley, *Nature* **318,** 162 (1985).

[5]S. C. O'Brien, J. R. Heath, R. F. Curl, and R. E. Smalley, *J. Chem. Phys.* **88,** 220 (1988).

[6]J. R. Heath, R. F. Curl, and R. E. Smalley, *J. Chem. Phys.* **87,** 4236 (1987).

[7]R. F. Curl and R. E. Smalley, *Science,* **242,** 1017 (1988).

[8]E. A. Rohlfing, D. M. Cox, and A. Kaldor, *J. Chem. Phys.* **81,** 3322 (1984).

[9]H. Kroto, *Science* **242,** 1139 (1988).

[10]R. E. Smalley, *Accts. Chem. Res.* **25,** 98 (1992).

[11]R. B. Fuller, "Inventions: The Patented Works of Buckminster Fuller" St. Martin's Press, New York, 1983.

[12]W. Kratschmer, L. D. Lamb, K. Fostiropoulos, and D. R. Huffman, *Nature* **347,** 354 (1990).

[13]H. Yonehara and C. Pac, *Appl. Phys. Lett.* **61,** 575 (1992).

[14]Y. Wang, *Nature* **356,** 585 (1992).

[15]B. Miller, J. M. Rosamilia, G. Dabbagh, R. Tycko, R. C. Haddon, A. J. Muller, W. Wilson, D. W. Murphy, and A. F. Hebard, *J. Am. Chem. Soc.* **113,** 6291 (1991).

[16]Y. Wang and L. T. Cheng, *J. Phys. Chem.* **96,** 1530 (1992).

[17]P. M. Allemand, K. C. Khemani, A. Koch, F. Wudl, K. Holczer, S. Donovan, G. Grüner, and J. D. Thompson, *Science* **253,** 301 (1991).

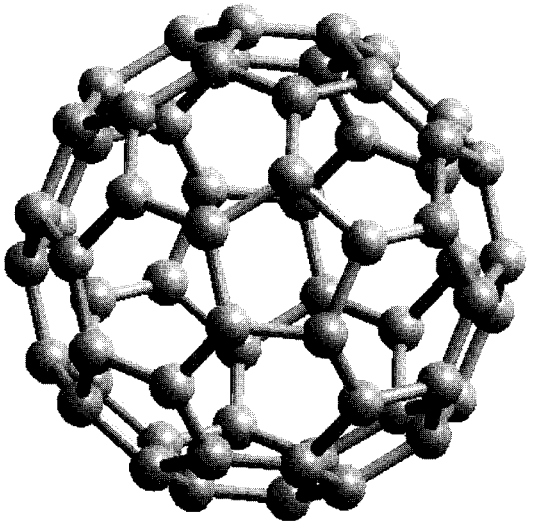

FIG. 1. Molecular structure of Buckminsterfullerene, C_{60}.

with an emphasis on the intensely studied materials K_3C_{60} and Rb_3C_{60}. Our goal is to provide condensed matter researchers with an up to date status report on the key properties of these new superconductors for which a reasonable consensus has been reached among researchers. In addition, we will comment on important open issues of fullerene superconductivity that await resolution. The structure of the chapter will be as follows: First, we will briefly review the structural and electronic properties of C_{60} and alkali metal–doped C_{60} solids. With this background information in hand, we will turn to a synopsis of normal state resistivity studies and a review of measurements of the critical fields, penetration depth, and coherence length in these materials. The role of sample granularity will also be discussed. Second, we will focus on investigations that directly address the microscopic mechanism of superconductivity in these new solids. We will begin this section with a brief overview of key models proposed to explain fullerene superconductivity. Within the context of these models, we will then overview (1) the dependence of T_c on lattice constant, (2) the energy gap, (3) phonons, and (4) the isotope effect. Throughout this chapter we will assume that the reader has an introductory level understanding of classical superconductors.[18]

[18]M. Tikham, "Introduction to Superconductivity". McGraw-Hill, New York, 1975.

II. Normal and Superconducting State Phenomenology

1. Crystal and Electronic Structures

a. *Crystal Structures*

On the basis of extensive structural studies, it is now well established that solid C_{60} forms a face-centered cubic (fcc) lattice with a lattice constant of 14.17 Å at room temperature (Fig. 2).[19–25] In this structure the distance between nearest-neighbor C_{60} clusters is 10 Å, and thus the intercluster separation (diameter of $C_{60} = 7.1$ Å) is 2.9 Å. This intercluster separation is 0.45 Å less than the 3.35-Å interplanar separation in graphite. In addition, there are sizable empty holes, which constitute 26% of the total cell volume, within the fcc C_{60} lattice. There are two tetrahedral holes and one octahedral hole with radii of 1.12 and 2.06 Å, respectively, per C_{60} molecule. A more detailed account of the structural properties of solid C_{60} can be found in the chapter by Axe, Moss, and Neumann in this volume.

Early studies at Bell Laboratories showed that exposure of C_{60} to alkali metal vapor resulted in the uptake of alkali metal into the lattice with a concomitant increase in conductivity.[26] In the case of potassium, the potassium-doped fullerene solid was also found to exhibit superconductivity below 18 K.[1]

Although neither the stoichiometry nor structure of the superconducting phase was known initially, this group proposed that the potassium intercalated into the octahedral and/or tetrahedral holes in the lattice.

[19]J. E. Fischer, P. A. Heiney, and A. B. Smith, *Accts. Chem. Res.* **25,** 115 (1992).
[20]S. Liu, Y.-J. Lu, M. M. Kappes, and J. A. Ibers, *Science* **254,** 408 (1991).
[21]P. A. Heiney, J. E. Fisher, A. R. McGhie, W. J. Romanow, A. M. Denenstein, J. P. McCauley, and A. B. Smith, *Phys. Rev. Lett.* **66,** 2911 (1911).
[22]J. E. Fisher, P. A. Heiney, A. R. McGhie, W. J. Romanow, A. M. Denenstein, J. P. McCauley, and I. A. B. Smith, *Science* **252,** 1288 (1991).
[23]W. I. F. David, R. M. Ibberson, J. C. Matthewman, K. Prassides, T. J. S. Dennis, J. P. Hare, H. W. Kroto, R. Taylor, and D. R. M. Walton, *Nature* **353,** 147 (1991).
[24]D. A. Neumann, J. R. D. Copley, R. L. Cappelletti, W. A. Kamitakahara, R. M. Lindstrom, K. M. Creegan, D. M. Cox, W. J. Romanow, N. Coustel, J. P. McCauley, Jr., N. C. Maliszewskyj, J. E. Fischer, and A. B. Smith III, *Phys. Rev. Lett.* **67,** 3808 (1991).
[25]J. Q. Li, Z. X. Zhao, D. B. Zhu, Z. Z. Gan, and D. L. Yin, *Appl. Phys. Lett.* **59,** 3108 (1991).
[26]R. C. Haddon, A. F. Hebard, M. J. Rosseinsky, D. W. Murphy, S. J. Duclos, K. B. Lyons, B. Miller, J. M. Rosmilia, R. M. Fleming, A. R. Kortan, S. H. Glarum, A. V. Makhija, A. J. Muller, R. H. Eick, S. M. Zahurak, R. Tycko, G. Dabbagh, and F. A. Thiel, *Nature* **350,** 321 (1991).

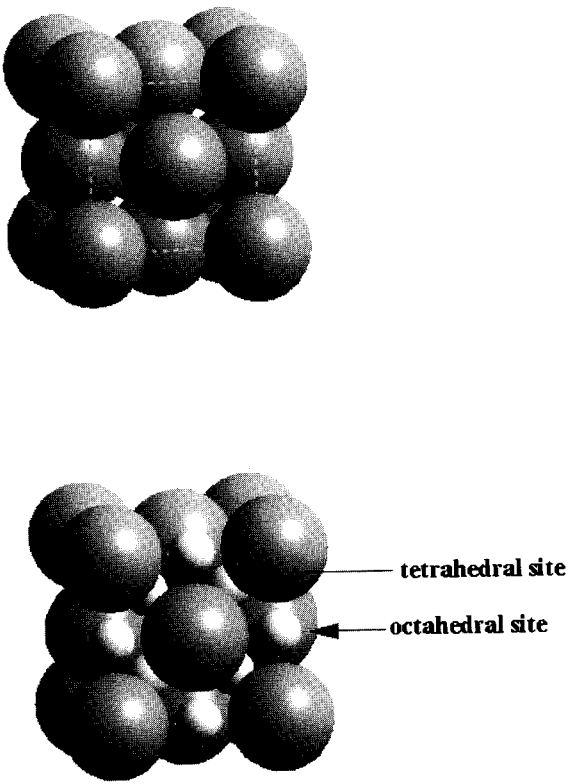

FIG. 2. Model illustrating the packing of individual fullerene clusters in the fcc lattice of solid C_{60} (top). Model illustrating the packing of alkali metal ions into the tetrahedral and octahedral holes in the fcc M_3C_{60} lattice (bottom). The C_{60} clusters are represented by gray shaded spheres and the alkali metal ions by smaller, light gray shaded spheres.

Subsequent studies have shown that the stoichiometries of the potassium[27,28] and rubidium-doped[29–31] C_{60} superconductors are K_3C_{60} and Rb_3C_{60}, respectively. Indeed, all of the known alkali metal–doped superconductors have the same M_3C_{60} stoichiometry. The structure of

[27]K. Holczer, O. Klein, S.-M. Huang, R. B. Kaner, K.-J. Fu, R. L. Whetten, and F. Diederich, *Science* **252,** 1154 (1991).

[28]P. W. Stephens, L. Mihaly, P. L. Lee, R. L. Whetten, S.-M. Huang, R. Kaner, F. Deiderich, and K. Holczer, *Nature* **351,** 632 (1991).

[29]C.-C. Chen, S. P. Kelty, and C. M. Lieber, *Science* **253,** 886 (1991).

[30]R. M. Fleming, A. P. Ramirez, M. J. Rosseinsky, D. W. Murphy, R. C. Haddon, S. M. Zahurak, and A. V. Makhija, *Nature* **352,** 787 (1991).

[31]P. W. Stephens, l. Mihaly, J. B. Wiley, S.-M. Huang, R. B. Kaner, F. Diederich, R. L. Whetten, and K. Holczer, *Phys. Rev. B* **45,** 543 (1992).

this M_3C_{60} phase was first elucidated by Stephens and coworkers[28] for K_3C_{60} and shown to be a simple derivative of the undoped fcc C_{60} solid. Specifically, the three alkali metal ions per C_{60} reside in the one octahedral and two tetrahedral holes in the lattice (Fig. 2).

The M_3C_{60} superconductors in contrast to the copper oxide materials, represent a structurally limited family of materials in that only the 3:1 stoichiometry is known to be conducting and superconducting (for alkali metals). Although there are other structurally known alkali metal–doped fullerene materials, such as the body-centered tetragonal (bct) phases M_4C_{60}[19,32] and the body-centered cubic (bcc) phase M_6C_{60},[19,33] these phases are insulating. The relatively simple structure and stoichiometry of the M_3C_{60} family of superconductors, however, does eliminate many of the problems of chemical inhomogeneity that have plagued physical measurements for the copper oxide superconductors. A summary of structurally characterized alkali metal–doped M_3C_{60} superconductors is given below in Table I. This table shows that there are a number of specific alkali metal–doped materials with the M_3C_{60} stoichiometry, where M is either a single alkali metal or mixture of alkali metals.[29,30,34–36] More recently, superconductivity has also been observed in the alkaline earth–metal–doped C_{60} materials Ca_5C_{60}[37] and Ba_6C_{60}.[38] To date, few physical measurements of the superconducting state properties of these new alkaline-earth metal–doped C_{60} solids have been made, and thus we will not discuss these materials further in this chapter.

b. *Electronic Structure*

The common structure and stoichiometry of the alkali metal–doped C_{60} superconductors indicates that a single picture can be used to describe the electronic structure of these materials. Here we briefly

[32]R. M. Fleming, M. J. Rosseinsky, A. P. Ramirez, D. W. Murphy, J. C. Tully, R. C. Haddon, T. Siegrist, R. Tycko, S. H. Glarum, P. Marsh, G. Dabbagh, S. M. Zahurak, A. V. Makhija, and C. Hampton, *Nature* **352,** 701 (1991).

[33]O. Zhou, J. E. Fischer, N. Coustel, S. Kycia, Q. Zhu, A. R. McGhie, W. J. Romanow, J. P. McCauley, A. B. Smith, and D. E. Cox, *Nature* **351,** 461 (1991).

[34]O. Zhou, R. M. Fleming, D. W. Murphy, M. J. Rosseinsky, A. P. Ramirez, R. B. van Dover, and R. C. Haddon, *Nature* **362,** 433 (1993).

[35]M. J. Rosseinsky, D. W. Murphy, R. M. Fleming, R. Tycko, A. P. Ramirez, T. Siegrist, G. Dabbagh, and S. E. Barrett, *Nature* **356,** 416 (1992).

[36]K. Tanigaki, I. Hirosawa, T. W. Ebbesen, J. Mizuki, Y. Shimakawa, Y. Kubo, J. S. Tsai, and S. Kuroshima, *Nature* **356,** 419 (1992).

[37]A. R. Kortan, N. Kopylov, S. Glarum, E. M. Gyorgy, A. P. Ramirez, R. M. Fleming, F. A. Thiel and R. C. Haddon, *Nature* **355,** 529 (1992).

[38]A. R. Kortan, N. Kopylov, S. Glarum, E. M. Gyorgy, A. P. Ramirez, R. M. Fleming, O. Zhou, F. A. Thiel, P. L. Trevor, and R. C. Haddon, *Nature* **360,** 566 (1992).

TABLE I. LATTICE CONSTANTS AND TRANSITION TEMPERATURES OF THE ALKALI METAL–DOPED C_{60} SUPERCONDUCTORS

MATERIAL	FCC LATTICE CONSTANT (Å)	T_c (K)
Na_2RbC_{60}	14.028	2.5
Na_2CsC_{60}	14.133	11
K_3C_{60}	14.253	19.2
K_2RbC_{60}	14.299	21.8
K_2CsC_{60}	14.292	24
KRb_2C_{60}	14.364	26
Rb_3C_{60}	14.436	29.4
$(NH_3)_4Na_2CsC_{60}$	14.473	29.6
Rb_2CsC_{60}	14.493	31.3

outline a simplified picture of the electronic structure of C_{60} and its solid compounds; the chapter by Pickett in this volume provides a detailed review of the electronic structure of these materials.

Because the interactions between individual C_{60} clusters within the solid are relatively weak (i.e., the closest intercluster distance is 2.9 Å) compared with the intracluster bonding, it is possible to obtain a useful picture by first considering the isolated molecular (cluster) states and then using these molecular orbitals to derive the energy bands and density of states for the bulk solid.[2] Qualitatively, the key features of the electronic structure of C_{60} can be derived by considering the atomic $p(\pi)$ orbitals that radiate from each of 60 equivalent carbon atoms. Semiempirical Hückel calculations provide the relative energy ordering of the molecular orbitals derived from these atomic π orbitals (Fig. 3). After filling these molecular orbitals with the 60 available π electrons, it is evident that C_{60} has a closed shell ground state where the highest occupied molecular orbital (HOMO) has h_u symmetry and contains 10 electrons, and the lowest unoccupied molecular orbital (LUMO) has t_{1u} symmetry and can hold up to 6 electrons.

The band structure and density of states can be inferred from this simple molecular orbital picture. Specifically, five valence bands are derived from the fivefold degenerate h_u-HOMO, and three conduction bands arise from the threefold degenerate LUMO of C_{60}. Details of the energy dispersions for these bands can be found in the chapter by Pickett in this volume. The insulating properties of solid C_{60} are thus a consequence of the fact that the h_u-derived bands are filled and the t_{1u} bands are empty. The gap in the density of states between the h_u-derived

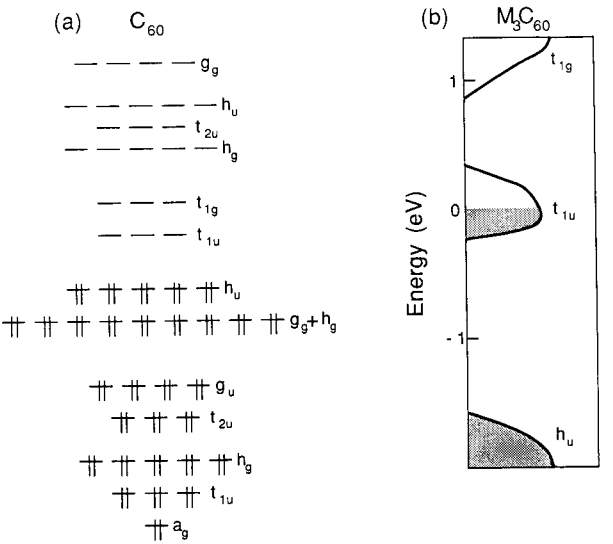

FIG. 3. (a) Hückel molecular orbital diagram that illustrates symmetry, degeneracy, and filling of the molecular orbitals on an individual C_{60} cluster. Electron pairs filling individual states are indicated by pairs of vertical parallel lines. (b) Schematic diagram of the density of states for M_3C_{60} solid in which C_{60} is orientationally disordered. The t_{1u} derived energy band is half-filled.

valence and the t_{1u}-derived conduction bands in solid C_{60} is approximately 1.7 eV.[39]

The dramatic increase in conductivity upon doping solid Buckminsterfullerene with three alkali metals per C_{60} is readily explicable in terms of the basic picture that has been presented. Specifically, the alkali metal dopants donate charge ($1e^-$/metal) to the t_{1u}-derived energy bands since an alkali metal s orbital (e.g., K 4s) lies significantly higher in energy than the t_{1u}-derived conduction bands. The M_3C_{60} materials are thus metals with a half-filled t_{1u} band.[40–44] A schematic illustration of the density of states illustrating this point is shown in Fig. 3. In addition, it is readily evident using this simple model why the M_6C_{60} materials are insulators: The t_{1u}-derived band becomes filled with the donation of six

[39]S. Saito and A. Oshiyama, *Phys. Rev. Lett.* **66,** 2637 (1991).
[40]S. C. Erwin and W. E. Pickett, *Science* **254,** 842 (1991).
[41]D. L. Novikov, V. A. Gubanov, and A. J. Freeman, *Physica C* **191,** 399 (1992).
[42]M. P. Gelfand and J. P. Lu, *Phys. Rev. Lett.* **68,** 1050 (1992).
[43]J. L. Martins and N. Troullier, *Phys. Rev. B* **46,** 1766 (1992).
[44]S. Satpathy, V. P. Antropov, O. K. Andersen, O. Jepsen, O. Gunnarsson, and A. I. Liechtenstein, *Phys. Rev. B* **46,** 1773 (1992).

electrons per C_{60}.[45] The insulating properties of M_4C_{60}, however, cannot be explained by this simple picture (i.e., it should be metallic).

To summarize, alkali metal doping is believed to result in complete charge transfer and a half-filled t_{1u}-derived band for the M_3C_{60} superconducting stoichiometry. Importantly, the width of this band is expected to be narrow since there is only weak overlap between adjacent C_{60} clusters within the lattice. Theoretical calculations have suggested that the bandwidth is approximately 0.6 eV.[40] Experimental determinations of this important parameter have yielded considerably greater uncertainty, with estimates ranging from 0.1 to >1 eV.[46–51] Because the bandwidth has important implications for the mechanism of superconductivity in these materials (to be discussed), it remains an important objective of experimental research to determine unambiguously the width of the t_{1u}-derived energy band.

2. Conductivity and Dimensionality

Resistivity and magnetoresistance measurements have played an important, but often controversial, role in determining details of the normal and superconducting states of the M_3C_{60} materials.[26,52–55] To date, much of this work has been carried out using doped thin film materials.[26,52,55] The first resistivity measurements on K-doped C_{60} films found a minimum of 2–5 mΩ cm at room temperature.[26] Upon cooling these films, the resistivity increases ca. 2× before undergoing a transition to a zero resistance state at 5 K. The transition temperature determined by

[45]S. C. Erwin and M. R. Pederson, *Phys. Rev. Lett.* **67,** 1610 (1991).

[46]C. T. Chen, L. H. Tjeng, P. Rudolf, G. Meigs, J. E. Rowe, J. Chen, J. P. McCauley, Jr., A. B. Smith III, A. R. McGhie, W. J. Romanow, and E. W. Plummer, *Nature* **352,** 603 (1991).

[47]P. J. Benning, F. Stepniak, D. M. Poirier, J. L. Martins, J. H. Weaver, L. P. F. Chibante, and R. E. Smalley, *Phys. Rev. B* **47,** 13843 (1993).

[48]G. K. Wertheim and D. N. E. Buchanan, *Phys. Rev. B* **47,** 12912 (1993).

[49]P. J. Benning, J. L. Martins, J. H. Weaver, L. P. F. Chibante, and R. E. Smalley, *Science* **252,** 1417 (1991).

[50]G. Sparn, J. D. Thompson, S.-M. Huang, R. B. Kaner, F. Diederich, R. L. Whetten, G. Grüner, and K. Holczer, *Science* **252,** 1829 (1991).

[51]L. D. Rotter, Z. Schlesinger, J. P. McCauley, Jr., N. Coustel, J. E. Fischer, and A. B. Smith III, *Nature* **355,** 532 (1992).

[52]G. P. Kochanski, A. F. Hebard, R. C. Haddon, and A. T. Fiory, *Science* **255,** 184 (1992).

[53]X.-D. Xiang, J. G. Hou, G. Briceño, W. A. Vareka, R. Mostovoy, A. Zettl, V. H. Crespi, and M. L. Cohen, *Science* **256,** 1190 (1992).

[54]X.-D. Xiang, J. G. Hou, V. H. Crespi, A. Zettl, and M. L. Cohen, *Nature* **361,** 54 (1993).

[55]T. T. M. Palstra, R. C. Haddon, A. F. Hebard, and J. Zaanen, *Phys. Rev. Lett.* **68,** 1054 (1992).

magnetization measurements, however, is significantly higher, 19.2 K. There are two important implications of these studies. First, even the most conducting samples are close to the Mott metal/insulator limit. Second, the T_c's determined by resistivity measurements may be reduced by film granularity. Further analysis of these initial data is not warranted, however, due to the uncertainty in sample quality (e.g., stoichiometry and crystallinity).

More recently, the Bell Laboratories group has carried out two detailed transport studies of potassium-doped C_{60} films prepared under carefully controlled ultrahigh vacuum conditions.[52,55] First, Kochanski and coworkers have prepared a series of K_xC_{60} ($x = 1$–6) films in which the value of x was determined to ±2% and the crystalline grain size was 60 Å.[52] In agreement with the earlier work, they found that the minimum resistivity in the films was 2.2 mΩ cm and showed that this corresponded to the doping level appropriate for the superconducting phase, $x = 3$. Assuming that there is complete charge transfer and thus three carriers per C_{60}, the effective scattering time, τ, can be written as

$$\tau = m/\rho n e^2 \tag{2.1}$$

and is of the order 10^{-15} sec. This yields an apparent mean free path, $l = v_f\tau$, of only 2 Å using the theoretically derived[40] Fermi velocity (v_f) of 2×10^{-7} cm/sec. Because this mean free path is significantly less than the intercluster separation (10 Å), this analysis is probably an inadequate explanation of the relatively high resistivity in these materials.

An alternative analysis of these transport data assumes that conductivity is dominated by the granularity of the system. This idea is reasonable since (1) the grain size in the polycrystalline thin films is small (≈60 Å) and (2) alkali metal doping naturally leads to insulating phases surrounding conducting K_3C_{60} grains. Within this framework, conduction is activated due to the charging energy, E_c. Because potassium doping ($x = 0$–6) changes the conducting grain size, E_c will also depend on x:

$$E_c = \frac{e^2}{2\pi\varepsilon D}\frac{2D}{d + 2\delta}, \tag{2.2}$$

where D is the grain size and δ is the gap between grains. The resistivity depends exponentially on E_c:[52,56]

$$\rho \propto \exp(E_c/2kT). \tag{2.3}$$

[56]B. Abeles, *Appl. Solid State Sci.* **6**, 1 (1976).

This model provides a good fit to the experimental data of Kochanski and coworkers, and it yields a grain size at $x = 3$ of 75 Å. The close agreement of this value with grain size determined by x-ray diffraction strongly supports the validity of this interpretation by the Bell Laboratories group. These results suggest that it will be important to account for sample granularity in the analysis of critical parameters of the superconducting state.

The thin film resistivity data for K_3C_{60} has also been used to investigate the dimensionality of this system.[55] Above, T_c, superconducting fluctuations may be observed as an excess in the normal state conductivity (paraconductivity, σ'). The scaling of the paraconductivity near T_c is strongly dependent on the dimensionality and can thus be used to assess this important idea:

$$\sigma' \propto t^{(d-4)/2}, \tag{2.4}$$

where $t = (T - T_c)/T_c$ and d is the dimension of the system.[57,58] Plots of $\log \sigma'$ vs. $\log t$ yield a straight line with slope $= -2$ for $t < 0.4$, and thus the critical dimension of the system is zero. For $t > 0.4$, which corresponds to temperatures greater than the T_c derived from magnetic measurements, there is, however, a crossover to 3D behavior. Notably, zero-dimensional fluctuations are the signature of weakly coupled superconducting grains, and thus this analysis is completely consistent with the granular picture derived from doping studies of K_xC_{60}.[52]

An important issue regarding studies of thin film (and polycrystalline bulk) samples that should be addressed in the future is whether granularity is intrinsic to these materials. For example , can single-crystal-like films be grown at elevated temperatures, and if so, can such films be doped homogeneously? It may be that the process of doping, which initially proceeds through the formation of C_{60}, M_3C_{60}, and M_6C_{60} phases, intrinsically leads to granular materials. The development of better quality thin film materials will undoubtedly lead to a deeper understanding of the intrinsic properties of these materials.

A somewhat different picture of the conductivity has been inferred from transport measurements made on K- and Rb-doped C_{60} single crystals by Zettl and coworkers.[53,54] First, they have found that the resistivity decreases with decreasing temperature from 300 K to T_c, and second, they have determined that the T_c's determined from these data are the same (not lower) than those determined magnetically for K_3C_{60} and Rb_3C_{60}. Initial analyses of σ' for a K-doped sample showed no

[57]W. J. Skocpol and M. Tinkham, *Rep. Prog. Phys.* **38,** 1049 (1975).
[58]L. G. Aslamasov and A. I. Larkin, *Phys. Lett. A* **26,** 238 (1968).

evidence for fluctuation effects near T_c, although in a later study both K- and Rb-doped C_{60} materials were reported to show fluctuation conductivity. Analysis of the excess conductivity using the Aslamazo and Larkin[57,58] scaling relation (Eq. 2.3) and the Maki–Thompson[59] expression (which also considers pair breaking effects) leads to the conclusion that both materials are 3D conductors/superconductors; there is no evidence for granularity in their data.

These single crystal data seem to indicate that granularity in the film measurements is not intrinsic to the M_3C_{60} materials. There are, however, several caveats to the crystal results. First, the absolute room-temperature resistivity of the single crystals is about the same, 2 mΩ cm, as that determined in the granular films. In addition, the stoichiometry and doping homogeneity of the single crystals have not been addressed. In the future it will be important to determine the stoichiometry and the fraction of bulk superconducting material. This latter point might be addressed via magnetization measurements. Last, although transport in the thin film samples appear to differ significantly (0D vs. 3D) from the single crystals, it is interesting to note that the crossover to 3D fluctuation effects in the thin films occurs in the same temperature range in which 3D fluctuations are observed in the single crystals. To summarize, these thin film and single crystal data indicate that in the limit of ideal samples M_3C_{60} behaves as 3D metal; however, for most practical thin film and bulk samples studied to date, sample granularity must be accounted for in the analysis of the normal state and superconducting state data.

3. Critical Fields, Penetration Depth, and Coherence Length

The upper and lower critical fields (H_{c2} and H_{c1}, respectively), the magnetic penetration depth (λ), and the superconducting pair coherence length (ξ) are parameters essential to characterizing any superconductor. Here we will review several studies that have addressed these critical parameters in K_3C_{60} and Rb_3C_{60} materials. The general picture to emerge from this work is that the metal-doped fullerene materials are extreme type II superconductors, $\kappa = \lambda/\xi \gg 1$, and in this regard are very much like the high temperature copper oxide superconductors.

The first measurements of H_{c2} and H_{c1} were made on K_3C_{60} materials by Holczer and coworkers.[60] They carried out temperature-dependent

[59]K. Maki and R. S. Thompson, *Phys. Rev. B* **39**, 2767 (1989).

[60]K. Holczer, O. Klein, G. Grüner, J. D. Thompson, F. Diederich, and R. L. Whetten, *Phys. Rev. Lett.* **67**, 271 (1991).

dc-magnetization studies of bulk polycrystalline K_3C_{60} samples at fields up to 5 T. The upper critical field at $T = 0$, $H_{c2}(0)$, was then determined from an extrapolation using the Werthamer–Helfand–Hohenberg (WHH) expression[61]

$$H_{c2}(0) = 0.69 \left. \frac{\partial H_{c2}}{\partial T} \right|_{T_c} T_c, \tag{3.1}$$

This extrapolation yields $H_{c2}(0) = 50$ T.

The upper critical field corresponds to a field at which there is one flux quantum, Φ_0, per region of a Copper pair. Hence, H_{c2} provides a direct measure of critical length scale for the superconducting state:

$$H_{c2} = \frac{\Phi_0}{2\pi\xi_{GL}^2}, \tag{3.2}$$

where ξ_{GL} is the Ginzburg–Landau coherence length. Using the extrapolated upper critical field, one finds that $\xi_{GL} = 25$ Å. Hence, the coherence length in the alkali metal–doped fullerene superconductors appear to be short and comparable with the values obtained for 2D copper oxide materials and not other 3D metals such as Nb (ξ(Nb) = 400 Å).

In addition, Holczer and coworkers carried out an analysis of their low-field data on the K_3C_{60} samples to determine H_{c1} and λ. The lower critical field at $T = 0$, $H_{c1}(0)$, obtained by extrapolating H_{c1} vs. T using the empirical relation

$$h_{c1}(T) = H_{c1}(0)[1 - (T/T_c)^2], \tag{3.3}$$

was ca. 130 Oe. The penetration depth can then be determined from $H_{c1}(0)$ and ξ using[18]

$$H_{c1}(0) = \frac{\Phi_0}{4\pi\lambda^2} \ln\left(\frac{\lambda}{\xi}\right) \tag{3.4}$$

This expression yields a value for $\lambda(0) = 2400$ Å. Hence, $\kappa = 96$, justifying the assertion that the M_3C_{60} materials are extreme type II superconductors.

There are, however, several important comments to make about the foregoing values of H_{c1}, H_{c2}, λ, and ξ_{GL}. First, the data used to obtain $H_{c2}(0)$ cover a limited range of fields relative to the extrapolated value. Second, in the case of $H_{c1}(0)$ it is difficult to assign unambiguously the values of H_{c1}(T) since the M vs. H data defines a nearly parbolic curve at

[61]N. R. Werthamer, E. Helfand, and P. C. Hohenberg, *Phys. Rev.* **147,** 295 (1966).

low fields rather than the expected linear one.[62] Third, sample granularity, which can affect significantly the measured values of H_{c2} and H_{c1}, was not accounted for in these studies.

The first serious attempt to account for sample granularity was made by Palstra and coworkers at Bell Laboratories.[55] Analysis of magnetoresistance measurements made in fields up to 12.5 T (2.5 × larger than used in the magnetization studies) using (3.1) results in an extrapolated upper critical field $H_{c2}(0) \approx 47$ T and a Ginzburg–Landau coherence length $\xi_{GL} = 26$ Å. While these results agree quite well with the magnetization studies, it was also recognized that the sample granularity enhances the observed upper critical field. Specifically, in the clean limit (mean free path, $l \gg \xi$), $\xi_{GL} = \xi_0$, where ξ_0 is the Pippard coherence length. In the dirty limit, however, the Ginzburg–Landau coherence length is reduced by the short mean free path of the conduction electrons:

$$\xi_{GL} = 0.85(\xi_0 \cdot l)^{1/2}. \tag{3.5}$$

Assuming that the critical field is a property of single grains, Palstra and coworkers determined that $\xi_0 \approx 150$ Å.

Finally, the penetration depth has also been estimated from other measurements. Uemura and coworkers[63] have used muon spin relaxation (μSR) measurements to determine λ as $T \to 0$.[63] In contrast to previous magnetization measurements, μSR is a relatively direct probe of the penetration depth since the μSR relaxation rate, σ, which is determined directly from experiment, is proportional to the inverse square of the penetration depth, λ^{-2}. Studies of polycrystalline K_3C_{60} samples yield $\lambda(0) \approx 4800$ Å.[63] This value is nearly two times larger than that determined from dc-magnetization measurements. Infrared reflectivity measurements made in the normal and superconducting states have also been used to estimate λ.[51,64] Studies from two different groups yield values of 5000 ± 1000 Å[51] and 8000 ± 500 Å.[64] These values of λ are consistent with extreme type II behavior, although clearly a consensus has not yet been reached for the value of the penetration depth.

Summarizing this section, the M_3C_{60} materials are extreme type II superconductors. These materials have upper critical fields as large as 50 T and correspondingly short coherence lengths with $\xi_{GL}(0) \approx 25$ Å. In

[62]V. Buntar, U. Eckern, and C. Politis, *Mod. Phys. Lett. B* **136,** 1037 (1992).

[63]Y. J. Uemura, A. Keren, L. P. Le, G. M. Luke, B. J. Sternlieb, W. D. Wu, J. H. Brewer, R. L. Whetten, S. M. Huang, S. Lin, R. B. Kaner, F. Diederich, S. Donovan, G. Grüner, and K. Holczer, *Nature* **352,** 605 (1991).

[64]L. Degiorgi, P. Wachter, G. Grüner, S.-M. Huang, J. Wiley, and R. B. Kaner, *Phys. Rev. Lett.* **69,** 1992.

addition, the magnetic penetration depth is large, ranging from 2400 to 8000 Å. Uncertainty in these length scales is likely due to variable sample quality (i.e., doping inhomogeneity) and granular effects. In the future, it will be important to improve these measurements using higher quality samples so that the intrinsic material properties can be unambiguously defined.

III. Mechanisms and Other Physical Properties

In Section II we reviewed the normal and superconducting state phenomenology of the alkali metal–doped fullerene superconductors. For the remainder of this chapter we will focus on experimental and theoretical studies of the microscopic mechanism of superconductivity in the M_3C_{60} materials. First, theoretical models based on electron–phonon- and electron–electron-mediated pairing will be introduced. Our emphasis will be to highlight features of these models that can be tested experimentally. The remaining sections of the chapter will then review key experimental studies that help to distinguish between the proposed theoretical models

4. Models for Fullerene Superconductivity

Theoretical models put forth to explain superconductivity in the fullerenes range from the conventional electron–phonon-mediated pairing model of Bardeen, Copper, and Schreiffer (BCS)[65–72] to models in which pairing is mediated by electron correlation effects.[73–77]

[65]J. Bardeen, L. N. Cooper, and J. R. Schrieffer, *Phys. Rev.* **108,** 1175 (1957).
[66]C. M. Varma, J. Zaanen, and K. Raghavachari, *Science* **254,** 989 (1991).
[67]M. Schluter, M. Lannoo, M. Needels, G. A. Baraff, and D. Tománek, *Phys. Rev. Lett.* **68,** 526 (1992).
[68]I. I. Mazin, O. V. Dolgov, A. Golubov, and S. V. Shulga, *Phys. Rev. B* **47,** 538 (1993).
[69]I. I. Mazin, S. N. Rashkeev, V. P. Antropov, O. Jepsen, A. I. Liechtenstein, and O. K. Andersen, *Phys. Rev. B* **45,** 5114 (1992).
[70]V. Z. Kresin, *Phys. Rev. B* **46,** 14883 (1992).
[71]R. A. Jishi and M. S. Dresselhaus, *Phys. Rev. B* **45,** 2597 (1992).
[72]F. C. Zhang, M. Ogata, and T. M. Rice, *Phys. Rev. Lett.* **67,** 3452 (1991).
[73]S. Chakravarty, M. P. Gelfand, and S. Kivelson, *Science* **254,** 970 (1991).
[74]S. Chakravarty, S. A. Kivelson, M. I. Salkola, and S. Tewari, *Science* **256,** 1306 (1992).
[75]S. Chakravarty and S. Kivelson, *Europhys. Lett.* **16,** 751 (1991).
[76]S. R. White, S. Chakravarty, M. P. Gelfand, and S. A. Kivelson, *Phys. Rev. B* **45,** 5062 (1992).
[77]G. Baskaran and E. Tosatti, *Curr. Sci.* **61,** 33 (1991).

a. *Phonon-Mediated Pairing*

The transition temperature for the BCS model of superconductivity is represented by[65]

$$T_c = 1.6\omega_{ph} \exp(-1/(\lambda - \mu^*)) \tag{4.1}$$

in the weak-coupling limit where $\lambda \ll 1$. The electron-phonon coupling parameter $\lambda = N(E_F)V$, where $N(E_F)$ is the density of states at the Fermi level and V is the coupling matrix to phonons with characteristic energy ω_{ph}. T_c is reduced in real materials by electron–electron repulsion that is accounted for by the renormalized Coulomb pseudopotential, μ^*:[78,79]

$$\mu^* = \frac{\mu}{1 + \mu \ln(E/\omega_{ph})}, \tag{4.2}$$

where E is the smaller of the Fermi energy and the plasma frequency.

The weak-coupling BCS expression for T_c was also extended a number of years ago to strong coupling by Eliashberg[80] and McMillan.[81] A particularly useful expression developed by McMillan, which is valid for $\lambda \leq 1.5$, is

$$T_c = \frac{\langle\omega\rangle}{1.2} \exp\left(\frac{-1.04(1 + \lambda)}{\lambda - \mu^* - 0.62\lambda\mu^*}\right), \tag{4.3}$$

where $\langle\omega\rangle$ is a logarithmic average of the phonon frequencies.

Electron–phonon coupling has been used to describe successfully superconductivity in a number of metallic compounds including Al (weak coupling) and Pb (strong coupling). The alkali metal–doped fullerene materials possess many differences from conventional metals (e.g., narrow conduction bandwidths and high frequency phonons); however, electron–phonon models still represent one logical starting point to describe superconductivity. Electron–phonon models specific to the fullerene superconductors have focused on coupling mediated by (1) high frequency intramolecular modes,[66,67] (2) a combination of high frequency intramolecular and low frequency intercluster modes,[68] and (3) low

[78]P. Morel and P. W. Anderson, *Phys. Rev.* **125,** 1263 (1962).
[79]O. Gunnarsson and G. Zwicknagl, *Phys. Rev. Lett.* **69,** 957 (1992).
[80]G. M. Eliashberg, *Sov. Phys. JETP* **11,** 696 (1960).
[81]W. L. McMillan, *Phys. Rev.* **167,** 331 (1968).

frequency C_{60}/alkali-metal optical modes.[72] Here we briefly summarize key features of several of these models.

Varma and coworkers[66] have developed a model to determine electron–phonon coupling parameters from the properties of single C_{60} clusters, and they have used these results in conjunction with the McMillan equation (4.3) to calculate T_c.[66] They justify the treatment of only intramolecular vibrations by asserting that because the electron–phonon coupling is proportional to the bandwidth and the covalent splitting of C_{60} states (i.e., the intramolecular band) is of order 10 eV versus the intermolecular band width of $\approx$0.5 ev, the intramolecular electron–phonon coupling will dominate in these materials. Within the context of this assumption, they showed that the coupling constant could be written as

$$\lambda = \frac{5}{6} N(E_F) \sum_m \frac{g_m^2}{M\omega_m^2}, \tag{4.4}$$

where the sum is over m intramolecular vibrations and g_m is the mth intramolecular deformation potential. Using semiempirical quantum chemical calculations, they found that only the two highest frequency tangential H_g modes at 1428 and 1575 cm^{-1} couple strongly to electrons. From the relation (4.4) they estimated that $\lambda = 0.3$–0.9, where the spread arises from uncertainty in $N(E_F)$; this range of λ corresponds to intermediate strength coupling. Finally, Varma and coworkers also investigated the dependence of T_c on $N(E_F)$ using their calculated value of λ and estimates for μ^*. An essential prediction of this analysis is that T_c should depend linearly on $N(E_F)$ for T_c above $\approx$20 K and $\mu^* \leq 0.2$.

A similar theoretical approach was also taken by Schluter and coworkers.[67] In this study, they considered only coupling to intramolecular phonons. They justified the neglect of intermolecular phonons in the pairing interaction with an argument similar to that by Varma *et al.* A combination of local density approximation–density functional and semiempirical tight binding calculations were used to evaluate the coupling matrix, $V_m = g_m^2/M\omega_m^2$ for eight H_g and two A_g intramolecular phonons. In contrast to Varma *et al.*, they found that there is significant coupling both to the lower frequency radial modes and the high frequency tangential modes; the overall λ ($= 5/6N(E_F \sum_m V_m)$ of 0.6 is, however, similar to the other work. Finally, it was pointed out that for the fullerene superconductors there is the unique situation that the electron–phonon coupling constant ($\lambda = N(E_F)V$) factors into an intercluster term $N(E_F)$, which is determined by the bandwidth, and the intramolecular term V, which is determined by single cluster phonon modes.

More recently, Mazin *et al.*[68] have proposed a somewhat different strong-coupling electron–phonon model.[68] In contrast to Varma and coworkers[66] and Schluter *et al.*,[67] they propose that coupling is mediated by both the high frequency intramolecular phonons ($\omega_{hf} \approx 1000\,cm^{-1}$) and very low frequency intermolecular modes ($\omega_{lf} \approx 40\,cm^{-1}$). In this "two-peak model," the electron–phonon coupling constant is factored into two components, where there is very strong coupling to the low frequency modes, $\lambda_{lf} \approx 2.7$, and moderate coupling to the high frequency modes, $\lambda_{hf} \approx 0.5$. Furthermore, the high frequency coupling constant should factor into intramolecular (V) and intermolecular ($N(E_F)$) components, but the low frequency constant cannot be factored. The important point about this two-peak model is that the inclusion of strong coupling to a low frequency mode provides a means for consistently explaining many experimental results (as will be discussed).[63,82–86]

Last, it is important to comment on several questions raised regarding the applicability of phonon models in general.[87] First, for the narrow band ($W \approx 0.5\,eV$) fullerene superconductors, the Fermi energy ($E_F \approx W/2 \approx 2000\,cm^{-1}$) is comparable with the intramolecular phonon energy ($\omega_{ph} \approx 1500\,cm^{-1}$) proposed to mediate pairing. This leads to a breakdown of Migdal's approximation and thus the calculation of T_c.[82,88,89] Second, there is considerable controversy concerning appropriate values for the renormalized Coulomb pseudopotential, μ^*.[79] This parameter is essential for all calculations of T_c, and thus an unambiguous estimate of its value is clearly needed in the future.

b. *Electronic Models for Superconductivity*

A very different nonphonon approach for explaining superconductivity in the alkali metal–doped fullerenes centers on consideration of electron correlation effects in these materials.[73–75] This work is motivated in part by the fact that C_{60} is a narrow band material in which the important physics may be dominated by electron–electron interactions. Several explicit models have been developed to explain electron pairing and

[82]G. S. Boebinger, T. T. M. Palstra, A. Passner, M. J. Rosseinsky, D. W. Murphy, and I. I. Mazin, *Phys. Rev. B* **46,** 5876 (1992).
[83]Z. Zhang, C.-C. Chen, S. P. Kelty, H. Dai, and C. M. Lieber, *Nature* **353,** 333 (1991).
[84]Z. Zhang, C.-C. Chen, and C. M. Lieber, *Science* **254,** 1619 (1991).
[85]Z. Zhang and C. M. Lieber, *Mod. Phys. Lett. B* **5,** 1905 (1991).
[86]R. Tycko, G. Dabbagh, M. J. Rosseinsky, D. W. Murphy, A. P. Ramirez, and R. M. Fleming, *Phys. Rev. Lett.* **68,** 1912 (1992).
[87]P. W. Anderson, unpublished results.
[88]A. B. Migdal, *Sov. Phys. JETP* **7,** 996 (1958).
[89]M. Grabowski and L. J. Sham, *Phys. Rev. B* **29,** 6132 (1984).

superconductivity via electron–electron interactions;[73–77] however, we will illustrate the general features of these models by reviewing the work of Chakravarty and coworkers.[73]

The basic problem in any electron–electron-mediated pairing model is getting an effective attractive interaction between electrons despite their inherently repulsive microscopic interaction. Qualitatively, the underlying idea behind pair binding arises from the resonating valence bond (RVB) picture.[90] For a strongly correlated system, the RVB state implies a separation of spin and change such that the electron is composite object made up of two quasi-particles: an *eon* of charge e and no spin, and a spinon of spin 1/2 and no change.

Within the context of the RVB picture, Chakravarty and coworkers defined Φ_0 and $\Phi_n = \Phi_0 + E_n$ as the ground state energy of the neutral molecule (C_{60}) and the energy of the molecule with n electrons, respectively. The pair binding energy, E_{pair}, is then

$$E_{\text{pair}} = 2E_1 - E_2 = 2\Phi_1 - \Phi_2 - \Phi_0, \tag{4.5}$$

where $E_{\text{pair}} > 0$ implies an attractive pairing. In terms of charge–spin separation, the energy to add one electron to the molecule, $E_1 = \Phi_1 - \Phi_0$, is the sum of the eon creation energy, E_e, the spinon creation energy, E_s, and the eon–spinon interaction energy, V_{es}:

$$E_1 = E_e + E_s + V_{es}. \tag{4.6}$$

Similarly, the energy to add two electrons to the molecule in the spin-singlet state required for superconductivity is $2E_e$ under the assumption that the eon–eon and spinon–spinon interaction energies are negligible. Hence, the pair binding energy can be written

$$E_{\text{pair}} = 2(E_s + V_{es}), \tag{4.7}$$

and when $E_s + V_{es} > 0$ singlet pairing should be attractive. That is, the energy to add two electrons to one C_{60} is less than the energy to add a single electron to each of two clusters.

[90]P. W. Anderson, *Science* **235,** 1196 (1987).

Chakravarty and cowkers[73] have quantified this picture using the microscopic Hubbard model. In terms of the on-site Coulomb repulsion U, and the hopping matrix element t, the pair binding energy can be obtained using second-order perturbation theory:

$$E_p = -0.05U + 0.015\frac{U^2}{t} + \ldots. \tag{4.8}$$

Notably, for reasonable values of U and t they have found that $E_p > 0$; that is, pairing is attractive.

The attractive pairing energy suggests that electron correlation on C_{60} may give rise to superconductivity. Assuming that the conduction bandwidth W is large compared with E_p, the superconducting transition temperature can be expressed using a BCS-like expression:

$$T_c \propto \exp(-W/E_p), \tag{4.9}$$

where E_p plays a role similar to V in the electron–phonon models. An important prediction that can be inferred from this model is that T_c should respond to intermolecular perturbations (through W) and intramolecular changes (through E_p) independently of each other. Other predictions as well as criticisms of this model have been reviewed.[73,74]

5. Transition Temperature Versus Lattice Constant

Soon after the discovery of superconductivity in K_3C_{60} at 19 K,[1] two groups reported that Rb-doped C_{60}, Rb_xC_{60}, exhibited superconductivity at the remarkably high temperature of 29 K.[27,91] Subsequent studies reported simultaneously by our group[29] and Bell Laboratories[30] showed that K- and Rb-doped materials had the same stoichiometry (M_3C_{60}) and structure (Fig. 2). Studies of a series of $(K_{1-x}Rb_x)_3C_{60}$ have provided significant insight into the mechanism of superconductivity in these materials.

[91]M. J. Rosseinsky, A. P. Ramirez, S. H. Glarum, D. W. Murphy, R. C. Haddon, A. F. Hebard, T. T. M. Palstra, A. R. Kortan, S. M. Zahurak, and A. V. Makhija, *Phys. Rev. Lett.* **66**, 2830 (1991).

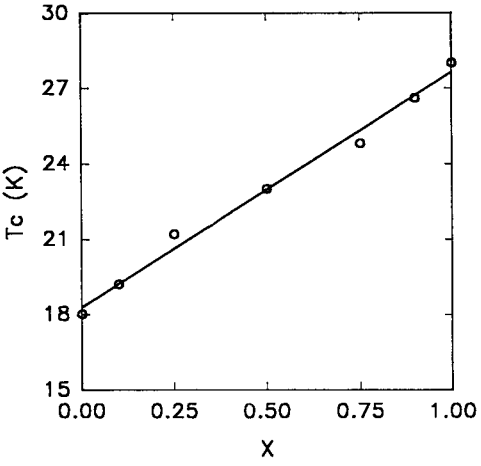

FIG. 4. Plot of T_c versus the Rb:K ratio x in $(K_{1-x}Rb_x)_3C_{60}$ solids. The fcc lattice constant increases from 14.253 to 14.436 as x increases from 0 to 1.

Chen and coworkers[29] found that T_c increased linearly with increasing x in an extensive series of $K_{1-x}Rb_x$-doped fullerene superconductors (Fig. 4). On the basis of these data Chen *et al.* suggested that substitution of Rb for K expands the fcc lattice (a "negative pressure" effect) and thereby systematically reduces the conduction bandwidth W. Because the total number of states in the t_{1u}-derived conduction band is constant, a reduction in W will increase $N(E_F)$. Hence, the linear relationship shown in Fig. 4 corresponds in effect to a systematic increase in T_c with increasing $N(E_F)$.

This picture was first quantified by the work of Fleming *et al.*[30] They found, in agreement with the work of Chen, that T_c increased linearly with the x, and they showed explicitly that T_c increased linearly with the fcc lattice constant, a_0. Fleming and coworkers further used semiempirical band structure calculations to estimate the density of states $N(E_F)$ as a function of a_0. They found an approximately 11% increase in $N(E_F)$ on going from K_3C_{60} to Rb_3C_{60}.

A number of additional experiments have been reported that are consistent with these results. First, Sparn *et al.*[50] and Schirber *et al.*[92] obtained related results from studies of the pressure dependence of T_c in polycrystalline K_3C_{60} materials. Both groups found that T_c decreased linearly with increasing pressures up to 20 kbar. The pressure coefficient,

[92]J. E. Schirber, D. L. Overmyer, H. H. Wang, J. M. Williams, K. D. Carlson, A. M. Kini, U. Welp, W.-K. Kwok, *Physica C* **178,** 137 (1991).

dT_c/dp, was similar in both studies: -0.78 and -0.63 K/kbar. In these studies, it was suggested that increasing pressure reduced the lattice constant monotonically, and that this reduction in lattice constant broadened W and reduced $N(E_F)$. An explicit calculation of the reduction in lattice constant with pressure, and consequently, the relationship between a_0 and T_c, was not made in these initial studies. Subsequent high pressure diffraction investigations of both K_3C_{60} and Rb_3C_{60} have determined the reduction in lattice constant with increasing pressure.[93] An analysis of these results seems to overlap reasonably well with the studies of the $(K_{1-x}Rb_x)_3C_{60}$ materials previously described. Hence, increasing pressure, which reduces a_0, will broaden the t_{1u}-derived conduction band and reduce $N(E_F)$.

In addition, there have been several measurements of $N(E_F)$ for K_3C_{60} and Rb_3C_{60} materials; these studies provide a direct check of the lattice constant effect proposed in the foregoing.[94,95] Tycko and coworkers[94] have used nuclear magnetic resonance (NMR) relaxation measurements to estimate the ratio of $N(E_F)$ for Rb_3C_{60} and K_3C_{60}.[94] Their analysis suggests that the Rb-doped material has 1.3–1.4 greater density of states at the Fermi level than K_3C_{60}. This observation is consistent with the calculations of Fleming *et al.*;[30] however, the magnitude of increase is $\approx$20% larger. Thermoelectric power measurements made on K- and Rb-doped crystals indicate that ratio of $N(E_F)$ for Rb:K is 1.5–1.8.[95] The increase in $N(E_F)$ is consistent with the trend suggested by the lattice constant studies; however, the absolute change is much larger. This large change suggests that the simple picture may not provide an adequate explanation of the observed results. Finally, we note the recent work of Zhou *et al.*,[34] who investigated the increase in T_c for Na_2CsC_{60} ($T_c = 10.5$ K) upon formation of an ammonia intercalation compound $(NH_3)_4Na_2CsC_{60}$ ($T_c = 29.6$ K).[34] The lattice constant of the $(NH_3)_4Na_2CsC_{60}$ compound, 14.47, is nearly the same as that of Rb_3C_{60} ($T_c = 29.2$ K). Despite the large chemical difference between these two compounds, their similar T_c values appear to be defined solely by the lattice constant or interaction between neighboring C_{60} clusters in the lattice.

The results that have been presented appear to provide strong support for the intramolecular electron–phonon mediated pairing models de-

[93]O. Zhou, G. B. M. Vaughan, Q. Zhu, J. E. Fischer, P. A. Heiney, N. Coustel, J. P. McCauley, Jr., and A. B. Smith III, *Science* **255,** 833 (1992).

[94]R. Tycko, G. Dabbagh, M. J. Rosseinsky, D. W. Murphy, R. M. Fleming, A. P. Ramirez, and J. C. Tully, *Science* **253,** 884 (1991).

[95]T. Inabe, H. Ogata, Y. Maruyama, Y. Achiba, S. Suzuki, K. Kikuchi, and I. Ikemoto, *Phys. Rev. Lett.* **69,** 3797 (1992).

scribed in Section 4. In these models, the expression for T_c factors the electron–phonon coupling constant λ into an intramolecular component V and an intermolecular component $N(E_F)$. In these models, the coupling matrix V is set by the intrinsic properties of single C_{60} clusters, and thus variations in T_c only arise from changes in $N(E_F)$. Hence, the changes in T_c due to variations in lattice constant[29,30] and pressure[50,92] support strongly these intramolecular phonon models. The results discussed here, however, also are completely consistent with pairing mediated by electron–electron correlation.[73–75] Specifically, the mean-field expression for T_c (relation (4.9)) in the electron correlation model is also factored into an intramolecular component (E_{pair}) and an intermolecular component (W). Since E_{pair} is determined by electron correlation on a single C_{60} cluster, variations in T_c for M_3C_{60} solids can be ascribed to variations in the bandwidth W. Because W and $N(E_F)$ depend similarly on lattice constant and pressure, the foregoing experimental studies cannot distinguish these fundamentally different models.

In addition, it is important to recognize that there are deviations from the linear relationship between T_c and the lattice constant. For example, Na_2CsC_{60} and Na_2RbC_{60} have been reported to have values of T_c of about 10 and 2.5 K, respectively.[35,36] Extrapolation of the T_c versus lattice constant results, previously described, to the measured lattice constants of these materials predicts higher values of T_c than determined experimentally. At present, these deviations cannot be explained by a simple factoring of the dependence of T_c into independent intramolecular and intermolecular contributions. The NMR[94] and thermoelectric power[95] measurements also deviate from the ideal intramolecular phonon picture since the large changes in the ratio of $N(E_F)$ suggest that low frequency phonons are also important in the pairing interaction. Clearly, further work will be needed to address these issues.

6. Energy Gap

The superconducting energy gap, 2Δ, is a measure of the energy scale binding Cooper pairs and thus is a parameter fundamental to models describing superconductivity in the alkali metal–doped fullerenes. Within the context weak coupling the BCS theory of superconductivity, it is possible to define a universal value for the reduced energy gap,

$$\frac{2\Delta}{kT_c} = 3.53, \tag{6.1}$$

that is independent of the details of the superconducting material.[65]

Correspondingly, values of 2Δ greater than $3.5kT_c$ indicate that the coupling is strong. Hence, measurements of 2Δ can be used to define the coupling regime for a material and thereby the appropriate energy scale of the excitations that mediate superconductivity. To date, the energy gap has been determined using a variety of techniques including tunneling,[83–85] infrared,[51,64,96] and NMR spectroscopies.[86] Here we will critically review the results from these different experiments.

a. *Tunneling*

Tunneling spectroscopy is a particularly attractive technique for probing the energy gap since the conductance, dI/dV, determined from current voltage, I–V, curves provides a direct measure of the density of states:

$$\frac{dI}{dV} = \int N_s(E) N_n |M|^2 \frac{df(E+eV)}{dV} dE, \tag{6.2}$$

where N_s is the density of states in the superconducting state, N_n is the normal state density of states, M is the tunneling matrix element, and $f(E)$ is the Fermi function.[97] In the limit of small bias and low temperature,

$$\frac{dI}{dV} \alpha N_s(E). \tag{6.3}$$

Zhang and coworkers[83–85] have used tunneling spectroscopy to investigate systematically the low energy electronic states in K_3C_{60} and Rb_3C_{60} polycrystalline superconductors.[83–85] Current–voltage curves recorded from 4.2 to 20 K on K_3C_{60} and from 4.2 to 30 K on Rb_3C_{60} samples were found to exhibit features characteristic of a superconducting energy gap (Fig. 5). At 4.2 K, where thermal broadening is minimized, the I–V curves exhibit low current near E_F and conductance onsets at $V \approx \pm 4$ and ± 6 meV for the K_3C_{60} and Rb_3C_{60} superconductors, respectively. Zhang and coworkers suggested that the conductance onsets corresponded to gap edges ($\pm\Delta$) in these materials.

Zhang *et al.* quantitatively assessed the magnitude of 2Δ for K- and

[96]S. A. FitzGerald, S. G. Kaplan, A. Rosenberg, A. J. Sievers, and R. A. S. McMordie, *Phys. Rev. B* **45**, 10165 (1992).

[97]E. L. Wolf, "Principles of Tunneling Spectroscopy." Oxford University Press, New York, 1989.

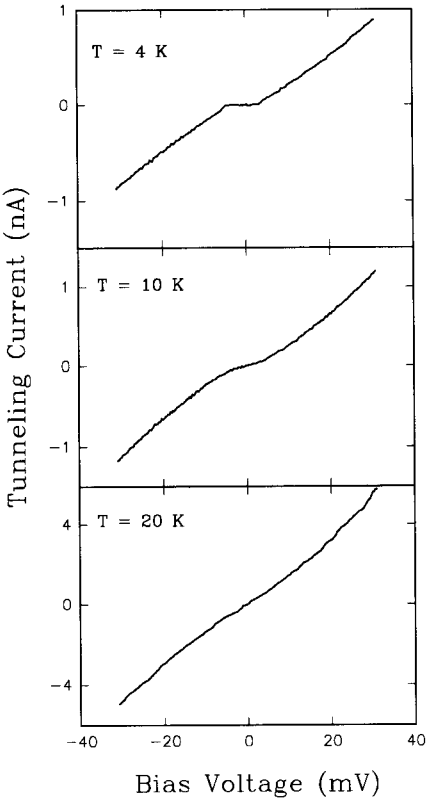

FIG. 5. Current versus voltage (I–V) curves recorded on a polycrystalline K_3C_{60} sample at 4.2, 10, and 20 K. The tunneling junction is a point contact and was formed using a low temperature scanning tunneling microscope.

Rb-doped materials by computing dI/dV and fitting the resulting curves to different models for N_s. They found that a BCS model for the density of states,[65]

$$N_s = \frac{eV}{[(eV)^2 - \Delta^2]^{1/2}}, \tag{6.4}$$

provided a poor fit to the data. Nevertheless, the value of 2Δ determined from this fit, $5.4kT_c$, was found to exceed significantly the BCS weak-coupling limit of $3.5kT_c$.

The poor agreement between the BCS model for N_s (6.4) and the experimental data was due to significant broadening in the latter. To account for this broadening and to obtain a more reliable estimate of 2Δ,

Zhang and coworkers also fit their data to the broadened density of states model proposed by Dynes:[98]

$$N_s = \mathrm{Re}\left\{\frac{|eV - i\Gamma|}{[(eV - i\Gamma)^2 - \Delta^2]^{1/2}}\right\}. \tag{6.5}$$

The Dynes model includes a parameter Γ to account for lifetime broadening near T_c. Formally, this model is not applicable to the low temperature data of Zhang *et al.* ($T/T_c < 0.25$), although they used it to account phenomenologically for broadening of an unknown origin. Examples of fits to the data of both the K_3C_{60} and Rb_3C_{60} superconductors at low temperature are shown in Fig. 6. From fits using this model they found that $2\Delta\ (K_3C_{60}) = 5.3kT_c$ and $2\Delta\,(Rb_3C_{60}) = 5.2kT_c$. Importantly, these values of 2Δ exceed significantly the weak coupling limit of $3.5kT_c$ and thus suggest that electrons may couple strongly to the relevant pairing excitations in the M_3C_{60} materials.

b. *Infrared*

The energy gap has also been probed in several infrared reflectance (IR) spectroscopy studies. Rotter *et al.*[51] first used IR spectroscopy to determine 2Δ in polycrystalline Rb_3C_{60} samples. The reflectivity spectra recorded above and below T_c showed changes expected for a superconductor, although the behavior was far from ideal. They defined the frequency at which the reflectivity ratio in the superconducting and normal states, R_s/R_n, dropped rapidly to be 2Δ; using this definition, $2\Delta = 3kT_c$–$5kT_c$. The considerable uncertainty in these results overlaps with both the weak-coupling BCS value for 2Δ and the larger value determined experimentally by tunneling spectroscopy. It is thus difficult to draw a strong conclusion from these results. More recently, a large range of 2Δ values, $2kT_c$–$5kT_c$, was reported on the basis of IR studies of K-doped C_{60} films.[96] Although no specific conclusion about the coupling strength can be made from these studies, the authors do make the important point that sample homogeneity must be improved to obtain conclusive results.

A somewhat different result has been reported by Degiorgi *et al.*,[64] who used IR reflectivity to determine the energy gap in K_3C_{60} and Rb_3C_{60} polycrystalline materials. They report that the optical reflectivity exhibits a well-defined gap feature that progressively sharpens as the temperature is reduced below T_c. These clean results contrast the ill-defined gap structure in the IR studies of Rotter *et al.*[51] and FitzGerald *et al.*,[96]

[98]R. C. Dynes, V. Narayanamurti, and J. P. Garno, *Phys. Rev. Lett.* **41,** 1509 (1978).

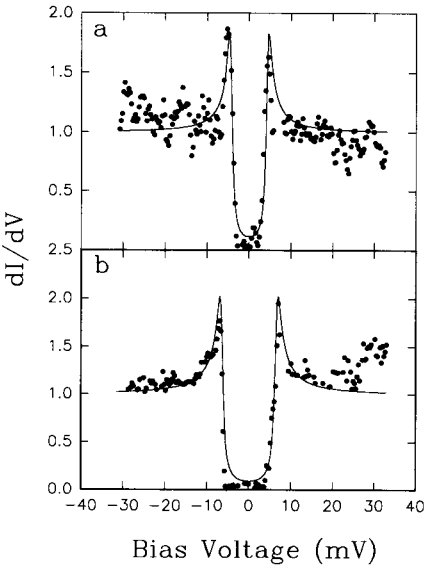

FIG. 6. Conductance (dI/dV) versus voltage curves for (a) K_3C_{60} and (b) Rb_3C_{60} at 4.2 K (filled circles). The solid lines correspond to best fits to relation (6.5) in the text. The values of the energy gap Δ and broadening function Γ in meV are $\Delta = 4.4$, $\Gamma = 0.5$ and $\Delta = 6.6$, $\Gamma = 0.6$ for K_3C_{60} and Rb_3C_{60}, respectively.

discussed already, and are believed to result from significantly improved sample quality. Notably, from the analysis of their reflectivity data Degiorgi and coworkers find that $2\Delta = 3.6kT_c$ and $3.0kT_c$ for the K_3C_{60} and Rb_3C_{60} materials, respectively. In contrast to the tunneling studies, these results appear to indiate that BCS-like weak-coupling models are appropriate for the fullerene superconductors. It is important to note, however, that the temperature dependence of the energy gap, $\Delta(T)$, determined in these IR studies deviates significantly from that predicted by BCS theory (to be discussed).

c. *NMR*

Finally, Tycko and coworkers[86] at Bell Laboratories have used NMR relaxation measurements to determine the magnitude of 2Δ in K_3C_{60} and Rb_3C_{60} superconductors. Fits of the ^{13}C-nuclear spin relaxation time, T_1, to an Arrhenius law,[99]

$$\frac{1}{T_1} = \omega \exp\left(-\frac{\Delta}{T}\right), \tag{6.6}$$

[99]L. C. Hebel and C. P. Slichter, *Phys. Rev.* **113,** 1504 (1959).

yield values of 2Δ for K_3C_{60} and Rb_3C_{60} of $3.0kT_c$ and $4.1kT_c$, respectively. These reported values of 2Δ appear to be consistent with the weak-coupling prediction of BCS theory [A recent calculation[70] based on these results yields values of λ for 2.1 and 1.5 for the Rb- and K-doped materials, respectively, and thus suggests strong coupling.]. There are important concerns regarding a weak-coupling interpretation of the NMR data. First, no Hebel–Slichter peak[99] was observed in the relaxation data. Because strongly coupled superconductors are not expected to exhibit a clear Hebel–Slichter peak, it is possible that NMR results are not clear evidence for weak coupling. Along these lines, it is interesting to note that NMR probes the minimum quasi-particle excitation energy. Therefore, when the gap is not clean, the value of 2Δ determined by NMR will be smaller than the true order parameter for the system. This same criticism also holds for IR spectroscopy and will be discussed further below.

d. *Implications*

The measurements of 2Δ reported to date range from $3kT_c$–$5kT_c$. In comparison with work at a similar stage on the copper oxide superconductors, these fullerene gap studies have a much better agreement. Since the results range from the weak-coupling to strong-coupling regimes, however, it may not be possible to use them to distinguish critically between proposed models for fullerene superconductivity at the present time.

We thus consider whether it is possible to develop a consistent picture from these results by considering the strengths and weaknesses of the individual measurement techniques. First, it is important to consider what the techniques measure and how the polycrystalline M_3C_{60} samples might influence these measurements. As discussed in Section 6.a, tunneling spectroscopy measures the conductance, which is proportional to N_s. Uncertainty in the value of 2Δ can arise from several sources, including (1) the model used to relate N_s and Δ and (2) inhomogeneity in the surface properties of the M_3C_{60} polycrystalline samples used to form the metal/insulator/superconductor junctions. The tunneling studies of Zhang *et al.* have shown that the magnitude of 2Δ is not very sensitive to the particular model chosen to relate N_s and Δ, although N_s is clearly broadened significantly relative to an ideal BCS model. The role of sample surface inhomogeneity, which could arise from degradation of the highly reactive M_3C_{60} surfaces, was not addressed in these studies. Degradation of the superconducting properties at the sample surface should not give rise to large values of 2Δ, however, but rather will

increase the conductance at zero bias voltage ($V = 0$). The relatively low conductance observed by Zhang and coworkers at $V = 0$ suggests that this (degradation) may not be a problem, although additional tunneling studies are needed to verify this work.

In contrast to tunneling spectroscopy, IR spectroscopy provides an onset frequency for the excitation of quasi-particles. In the studies we have discussed,[51,64,96] this onset was assigned to 2Δ. Uncertainty in the magnitude of 2Δ can arise from several sources, including (1) uncertainty in the onset of optical absorption and (2) the formal meaning of this optical onset. The optical onset is difficult to define since it corresponds to the deviation from 100% reflectivity. In the studies of Rotter *et al.*[51] and FitzGerald *et al.*,[96] this onset is hard to assign and thus leads to a large uncertainty in 2Δ. The report by Degiorgi and coworkers improves upon these earlier studies, since it appears to show a sharp deviation from 100% reflectivity. A more important point, which has not been addressed, is that the optical onset corresponds formally to an optical gap, ω_g. Only in the case of an ideal BCS superconductor does $\omega_g = 2\Delta$, where Δ is the order parameter that defines the energy scale for pair binding. More generally, ω_g will be less than 2Δ due to inelastic (pair breaking) scattering and/or other processes that allow for excitations at frequencies less than 2Δ.[100–102]

It is therefore interesting to consider whether the tunneling and optical data are in fact consistent but simply measure different properties (i.e., 2Δ vs. ω_g) of the M_3C_{60} superconducting state. An important indication from the IR data of Degiorgi and coworkers[64] that supports this idea is that the temperature dependence of their measured energy gap deviates strongly from the behavior predicted by BCS theory. They report that the gap opens sharply below T_c and exhibits only a weak temperature dependence. Notably, these results agree with predictions of pair breaking theory.[100–102] We have thus analyzed the previous tunneling data of Zhang and coworkers within the framework of pair breaking to explicitly determine 2Δ and ω_g, although the origin of scattering in the fullerenes is unknown. An example of a fit to N_s for Rb_3C_{60} is shown in Fig. 7. The fit to the tunneling data using this model is significantly better than observed in the previous reports[83,84] and yields $2\Delta = 5.2kT_c$ and $\omega_g = 4.0kT_c$. Notably, the value of ω_g determined from this analysis is similar to the onset reported by Degiorgi and coworkers.[64]

This analysis suggests that 2Δ may be significantly larger than $3.5kT_c$

[100]A. A. Abrikosov and L. P. Gorkov, *Sov. Phys. KETP* **12,** 1243 (1991).
[101]Y. Wada, *Rev. Mod. Phys.* **253** (1964).
[102]S. Skalski, O. Betheder-Matibet, and P. R. Weiss, *Phys. Rev.* **136,** 1500 (1964).

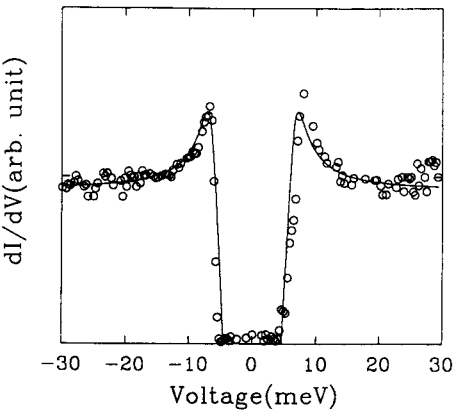

FIG. 7. Conductance (dI/dV) versus voltage data for Rb_3C_{60} at 4.2 K (open circles). The solid line corresponds to a best fit of the pair breaking model discussed in the text. The values of the energy gap Δ, optical gap ω_g, and pair breaking parameter α, are 6.6, 5.0, and 1.1 meV, respectively.

and is thus suggestive of strong coupling. Strong coupling constrains the electron–phonon models of superconductivity discussed in Section 4 in several ways. A large value of $2\Delta/kT_c$ would be inconsistent with models that consider only high frequency intramolecular phonons. Strong electron–phonon coupling with these high frequency modes would predict transition temperatures significantly higher than observed experimentally. The electron–phonon model that includes contributions from both high frequency intramolecular modes and low frequency intermolecular phonons,[68] however, would be consistent with the large values of $2\Delta/kT_c$. Finally, while these energy gap results may help to distinguish different electron–phonon models, they cannot, unfortunately, at present distinguish phonon-mediated pairing from the fundamentally different model based on pairing mediated by electron correlation.[73] Explicit predictions for the gap equation are needed for this latter model (e.g., how close the superconducting state is to a BCS-like one) in order to assess quantitatively its agreement with the experimental energy gap results.

7. PHONONS

One way in which to assess whether electron–phonon coupling or electron correlation is responsible for superconductivity is to investigate the coupling of different phonons to the conduction electrons. In solid

C_{60}, there are a number of phonon modes that should in principle be considered; these include (1) librational modes of C_{60} clusters in the lattice ($\omega = 15\,\text{cm}^{-1}$); (2) intermolecular C_{60}–C_{60} vibrational modes ($\omega \approx 40\,\text{cm}^{-1}$); (3) C_{60}–M^+ optical modes ($\omega \approx 60$–$100\,\text{cm}^{-1}$); and (4) radial and tangential intramolecular modes. The intramolecular radial modes can be characterized as low frequency (200–800 cm^{-1}), while the tangential modes are higher frequency (1000–1600 cm^{-1}). To date, most efforts have focused on the analysis of the radial and tangential intramolecular phonons,[103–110] since these modes are proposed to play a dominant role in intramolecular electron–phonon pairing models.

Symmetry analysis shows that only the eight H_g and two A_g intramolecular phonon modes can couple to the t_{1u} electronic states.[111] These modes, which are Raman active, have been studied by several groups using Raman and inelastic neutron scattering.[103–110] Duclos and coworkers[103] at Bell Laboratories have carried out Raman scattering experiments on C_{60}, M_3C_{60}, and M_6C_{60} (M = Na, K, Rb and Cs) to characterize the interaction of the Raman active modes with the conduction electrons. They found that K- and Rb-fullerene samples doped to the M_3C_{60} stoichiometry exhibit only three modes; these were the radial modes $H_g(1) = 265\,\text{cm}^{-1}$ and $A_g(1) = 497\,\text{cm}^{-1}$, and the tangential mode $A_g(2) = 1447\,\text{cm}^{-1}$. Interestingly, the $H_g(2)$ through $H_g(8)$ modes could not be detected in the spectra of the M_3C_{60} materials, although these phonons were clearly observed in pure C_{60} and M_6C_{60} solids. Duclos *et al.* suggest that the disappearance of the $H_g(2)$–$H_g(8)$ modes may be due to broadening of the spectral function as a result of electron–phonon coupling. They also note, however, that a decrease in the optical penetration depth, which occurs in the metallic M_3C_{60} state, could also explain the disappearance of these modes.

[103]S. J. Duclos, R. C. Haddon, S. Glarum, A. F. Hebard, and K. B. Lyons, *Science* **254,** 1625 (1991).

[104]M. G. Mitch, S. J. Chase and J. S. Lannin, *Phys. Rev. Lett.* **68,** 883 (1992).

[105]M. G. Mitch, S. J. Chase, and J. S. Lannin, *Phys. Rev. B* **46,** 3696 (1992).

[106]P. Zhou, K.-A. Wang, A. M. Rao, P. C. Eklund, G. Dresselhaus, and M. S. Dresselhaus, *Phys. Rev. B* **45,** 10838 (1992).

[107]P. Zhou, K.-A. Wang, Y. Wang, P. C. Eklund, M. S. Dresselhaus, G. Dresselhaus, and R. A. Jishi, *Phys. Rev. B* **46,** 2595 (1992).

[108]K.-A. Wang, Y. Wang, P. Zhou, J. M. Holden, S.-L. Ren, G. T. Hager, H. F. Ni, P. C. Eklund, G. Dresselhaus, and M. S. Dresselhaus, *Phys. Rev. B* **45** (1992).

[109]K. Prassides, J. Tomkinson, C. Christides, M. J. Rosseinsky, D. W. Murphy, and R. C. Haddon, *Nature* **354,** 462 (1991).

[110]K. Prassides, C. Christides, M. J. Rosseinsky, J. Tomkinson, D. W. Murphy, and R. C. Haddon, *Europhys. Lett.* **19,** 629 (1992).

[111]M. Lannoo, G. A. Baraff, M. Schluter, and D. Tomanek, *Phys. Rev. B* **44,** 1210 (1991).

Results similar to the study of Duclos *et al.* have also been reported by several other groups. Lannin and coworkers[104,105] have found significant broadening of the radial $H_g(2)$ and tangential $H_g(7)$ and $H_g(8)$ modes in Raman scattering studies of ultrathin Rb_xC_{60} thin films. These results suggests significant electron–phonon coupling only to three modes versus coupling to seven $H_g(2)$–$H_g(8)$ modes as reported by Duclos and coworkers. The Raman investigations of Zhou *et al.*[106] suggest a still different picture in that they find significant broadening of five radial and tangential H_g symmetry phonons in K_3C_{60} thin films. Finally, inelastic neutron scattering studies of C_{60} and K_3C_{60} have also been reported to show evidence for strong electron–phonon interactions.[109,110] Specifically, Prassides *et al.*[109,110] found that the $H_g(2)$ and $H_g(8)$ phonon modes disappeared in neutron scattering spectra of K_3C_{60}, and that the $H_g(1)$, $H_g(3)$, and $H_g(4)$ modes exhibited only small changes.

To summarize, Raman and inelastic neutron scattering experiments show significant spectral line broadening effects for several intramolecular H_g phonon modes. While studies reported to date do not agree on all of the specific modes that are broadened, there appears to be a consensus for at least the $H_g(2)$ and $H_g(8)$ phonon modes. Although it is reasonable to interpret these results as evidence supporting intramolecular electron–phonon-mediated pairing models for fullerene superconductivity, this interpretation should be made with caution. Electron–phonon coupling, as evidenced by spectral line broadening at fixed temperature, does not necessarily imply that these broadened phonons are important in superconductivity. Indeed, there will be electron–phonon interactions regardless of the mechanism of superconductivity. Only when the electron–phonon interaction is shown to affect the superconducting state is it reasonable to assert that phonons are responsible for pairing. In this regard, it would be interesting to investigate the Raman spectra of the M_3C_{60} superconductors as a function of temperature near T_c.[112] If the H_g modes really are responsible for pairing, they should exhibit changes in linewidth and intensity as the sample is cooled through the superconducting transition temperature.

8. Isotope Effect

A more direct method than those already discussed for investigating the role of phonons in superconductivity is to determine the magnitude of the shift in T_c upon isotopic substitution—the *isotope effect.* Historically,

[112]M. E. Flatté, *Phys. Rev. Lett.* **70,** 658 (1993); and M. E. Flatté, personal communication.

the observation of a suppression in T_c upon substitution of heavy isotopes of mercury in metallic mercury was a key result supporting phonon-mediated pairing as a mechanism for superconductivity.[113,114] For phonon-mediated pairing, the BCS model of superconductivity predicts that

$$T_c \propto M^{-\alpha}, \tag{8.1}$$

where M is the ionic mass and α is the isotope shift exponent. The ideal value of α predicted by BCS theory, 0.5, has been observed in a number of simple metals.[115] Corrections due, for example, to Coulomb interactions, however, will reduce the value of α below 0.5. Hence, measurements of the $^{13}C/^{12}C$ isotope effect in M_3C_{60} superconductors should provide a key test of the mechanism of superconductivity in the fullerenes.

Not surprisingly, there have been a number of experimental invesigations of the isotope effect in the M_3C_{60} materials.[116–120] In all cases, a significant isotope effect has been observed, although the range of reported values for α is large. Careful analysis of these results suggest that the intrinsic value of α for ^{13}C-substituted C_{60} is approximately 0.3.[116–118] Larger values of α have been observed in samples containing poorly controlled mixtures of $(^{13}C_{1-x}{}^{12}C_x)_{60}$ and $^{12}C_{60}$. In general, one expects that a simple mass average weighting should provide an accurate extrapolation of α to 100% substitution; however, the sensitivity of the M_3C_{60} T_c to impurities and the unique cluster properties of the C_{60} superconductor (to be discussed) makes this assumption questionable. In short, only homogeneous samples possessing sharp superconducting transitions can provide a good measure of the shift in T_c. The transition broadening that is often observed in small isotopically substituted samples[119,120] can easily lead to an overestimate of the shift in T_c, and thus to a large isotope effect.

Isotope shift measurements made in our laboratory at Harvard have

[113]C. A. Reynolds, B. Serin, W. H. Wright and L. B. Nesbitt, *Phys. Rev.* **78,** 487 (1950).
[114]E. Maxwell, *Phys. Rev.* **78,** 477 (1950).
[115]E. A. Lynton, "Superconductivity". Methuen, London, 1961.
[116]C.-C. Chen and C. M. Lieber, *J. Am. Chem. Soc.* **114,** 3141 (1992).
[117]C.-C. Chen and C. M. Lieber, *Science* **259,** 655 (1993).
[118]A. P. Ramirez, A. R. Kortan, M. J. Rosseinsky, S. J. Duclos, A. M. Mujsce, R. C. Haddon, D. W. Murphy, A. V. Makhija, S. M. Zahurak, and K. B. Lyons, *Phys. Rev. Lett.* **68,** 1058 (1992).
[119]T. W. Ebbesen, J. S. Tasi, K. Tanigaki, J. Tabuchi, Y. Shimakawa, Y. Kubo, I. Hirosawa, and J. Mizuki, *Nature* **355,** 620 (1992).
[120]A. A. Zakhidov, K. Imaeda, D. M. Petty, K. Yakushi, H. Inokuchi, K. Kikuchi, I. Ikemoto, S. Suzuki, and Y. Achiba, *Phys. Lett. A* **164,** 355 (1992).

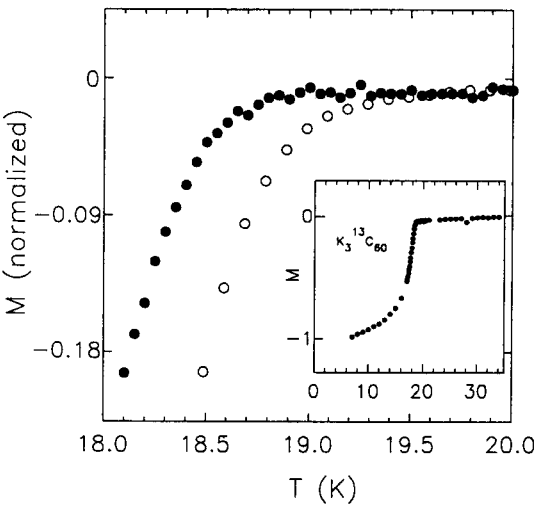

FIG. 8. High resolution temperature-dependent magnetization measurements on $K_3{}^{13}C_{60}$ (●) and $K_3{}^{12}C_{60}$ (○) samples highlighting the depression in T_c for the isotopically substituted material. The inset shows a full magnetization curve for a $K_3{}^{13}C_{60}$ sample.

avoided these experimental problems by focusing on homogeneous, 99.5% ^{13}C-substituted C_{60} solids.[116,117] An example of data obtained on a K_3C_{60} sample is shown in Fig. 8. Measurements made on both the $K_3{}^{13}C_{60}$ and $Rb_3{}^{13}C_{60}$ samples show unambiguously that the value of α for the fully substituted M_3C_{60} superconductors is 0.3.

With this reproducible result in hand, it is possible to evaluate the applicability of different models proposed to explain fullerene superconductivity. First, the observation of a significant isotope effect strongly supports the role of phonons in pairing. Using an expression derived from the McMillan equation (4.3), it is possible to evaluate whether intramolecular or intermolecular phonons are more likely to explain superconductivity in the fullerenes. Specifically, we can rewrite the McMillan equation expressing the isotope exponent α in terms of ω, λ, and μ^*:

$$\alpha = \frac{1}{2}\left\{1 - \left[\mu^* \ln \frac{\langle\omega\rangle}{1.2T_c}\right]^2 \frac{1+0.62\lambda}{1+\lambda}\right\} \tag{8.2}$$

Assuming high frequency intramolecular phonons are important and $\alpha = 0.3$, we find that $\lambda = 0.68$ and $\mu^* = 0.17$. If $\langle\omega\rangle$ is only made over the very low frequency intermolecular phonon modes, then $\lambda = 5$ and $\mu^* = 0.35$. In this latter case, the value of λ is outside the range for

which the McMillan relationship (8.2) is valid. This analysis thus indicates that high frequency intramolecular phonons may provide the most conventional parameter set for the experimentally observed isotope exponent of 0.3. Kresin[70] has also argued, however, that using a theory that properly accounts for strong coupling ($\lambda > 1.5$) can provide reasonable values of λ and μ^* (2 and 0.2, respectively) assuming that only low frequency modes are important.

There are two additional complications in the interpretation of these seemingly straightforward isotope effect experiments. First, Chakravarty and coworkers[74] have shown that it is also reasonable to expect a sizable isotope effect within the context of their electron correlation model of pairing.[74] The isotope effect in their model arises from the fact that the hopping matrix element t in relation (4.8) will increase upon ^{13}C-substitution due to a reduction in zero point fluctuation of the carbon–carbon bonds; that is, the mean C–C separation decreases upon isotopic substitution. Because the pair-binding energy is inversely related to t, T_c will decrease upon ^{13}C-substitution (see (4.8) and (4.9)). The estimated magnitude of the suppression in T_c for Rb_3C_{60} is 0.2 to 0.6 K, which yields α ranging from 0.08 to 0.25. Since the largest value of α approaches the experimental isotope exponent, it may be premature to rule out this electronic model on the basis of the experimental isotope effect.

Finally, we also mention the interesting experimental result of Chen *et al.*[117] To investigate the role of intramolecular and intermolecular

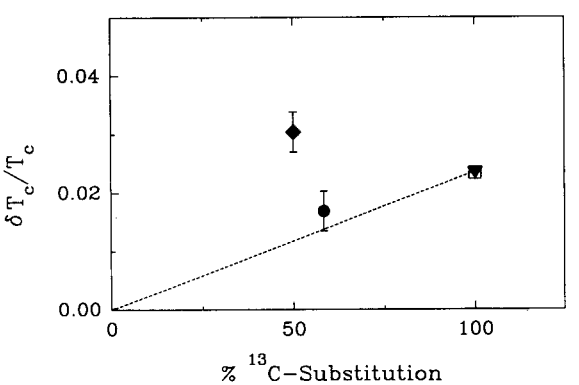

FIG. 9. Plot of the normalized isotope shift ($\delta T_c/T_c$) versus the percentage ^{13}C enrichment in the fullerene samples. The dashed line corresponds to the behavior expected for $\alpha = 0.3$. The experimental points are $Rb_3{}^{13}C_{60}$ (▼), $K_3{}^{13}C_{60}$ (□), $Rb_3(^{13}C_{.55}{}^{12}C_{.45})_{60}$ (●), and $Rb_3[(^{13}C_{60})_{.5}(^{12}C_{60})_{.5}]$ (◆). Notably, the isotope shifts observed for the $Rb_3[(^{13}C_{60})_{.5}(^{12}C_{60})_{.5}]$ samples are significantly larger than predicted for $\alpha = 0.3$.

phonons, they have prepared and studied a series of ^{13}C-substituted materials of the general form $Rb_3(^{13}C_{1-x}{}^{12}C_x)_{60}$ and $Rb_3[(^{13}C_{60})_{1-x}(^{12}C_{60})_x]$. In principle, these materials should exhibit the same isotope effect for a given value of x (assuming phonon-mediated pairing) since the materials have a similar weighted phonon density of states. Interestingly, Chen has reported that $Rb_3[(^{13}C_{60})_{1-x}(^{12}C_{60})_x]$ samples show an anomalously large isotope shift (Fig. 9). The origin of this interesting result is not known at present; however, we believe that a detailed explanation should provide critical insight into the mechanism of superconductivity in the alkali metal–doped fullerenes.

IV. Concluding Remarks

In this chapter we have attempted to provide a relatively comprehensive overview of the experimental status of the fullerene superconductors. We have emphasized (1) the normal state and superconducting state phenomenology as well as (2) experimental probes of the microscopic mechanism of superconductivity in these new molecular superconductors. As in any emerging field, there remains considerable uncertainty, and throughout this chapter we have tried to present a balanced review of accepted results and indicate where additional work is warranted. At present, many results point to a mechanism of electron–phonon-mediated pairing, but as indicated throughout Section III, electron correlation effects may still represent a viable explanation of superconductivity in these materials. Clearly, there is room (and a need) to explore more deeply the fascinating physics of these new superconductors.